

Green Chemistry

Accepted Manuscript



This is an *Accepted Manuscript*, which has been through the Royal Society of Chemistry peer review process and has been accepted for publication.

Accepted Manuscripts are published online shortly after acceptance, before technical editing, formatting and proof reading. Using this free service, authors can make their results available to the community, in citable form, before we publish the edited article. We will replace this *Accepted Manuscript* with the edited and formatted *Advance Article* as soon as it is available.

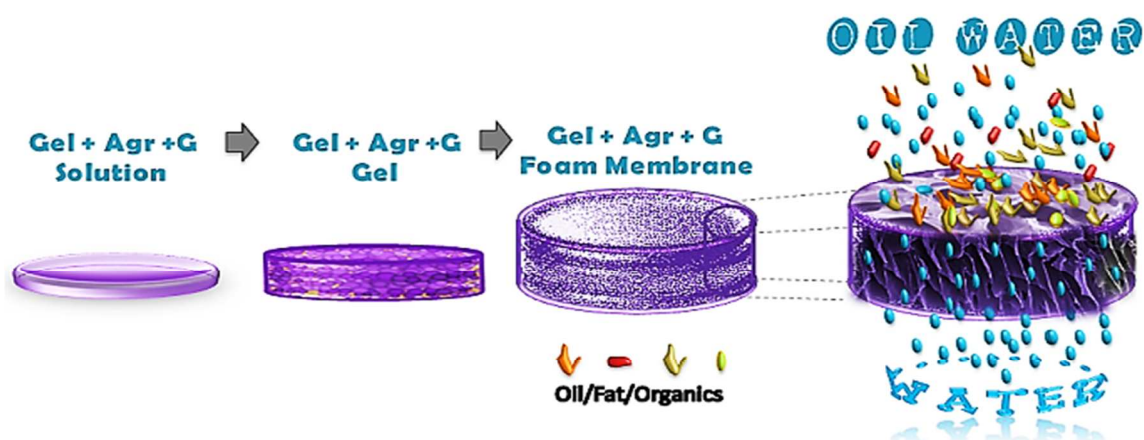
You can find more information about *Accepted Manuscripts* in the [Information for Authors](#).

Please note that technical editing may introduce minor changes to the text and/or graphics, which may alter content. The journal's standard [Terms & Conditions](#) and the [Ethical guidelines](#) still apply. In no event shall the Royal Society of Chemistry be held responsible for any errors or omissions in this *Accepted Manuscript* or any consequences arising from the use of any information it contains.



www.rsc.org/greenchem

Graphical Abstract



ARTICLE

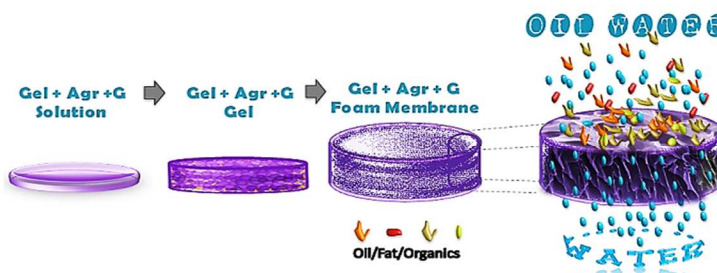
Bio-based super hydrophilic foam membranes for sustainable oil-water separation

Cite this: DOI: 10.1039/x0xx00000x

Jai Prakash Chaudhary,^a Sanna Kotrappanavar Nataraj,^{b*} Azaz Gogda^a and Ramavatar Meena^{a*}Received 00th January 2012,
Accepted 00th January 2012

DOI: 10.1039/x0xx00000x

www.rsc.org/



The development of a low cost high performance bio-based membrane technology has been attempted to clean harsh wastewater streams sensitive to environmental sustainability. Novel foam membranes (FMs) have derived from agarose (Agr) and gelatin (Gel) in combination with a non-toxic fruit extract natural crosslinker genipin (G). FMs were successfully tested for their oil-water separation efficiencies. FMs attained unique capillary microstructure (10-45 μm) as a result of controlled leophilization process, which allows selective permeation of water. Stable microporous membranes with nominal pore size covering the microfiltration and ultrafiltration range generated as high as $>500 \text{ L.m}^{-2}.\text{h}^{-1}$ continuous flux with $\sim 98\%$ pure product water. One of the advantages with FM, post oil-water separation is that it undergoes easy membrane cleaning process thereby retaining surface activity for long term performance.

1. Introduction

Last two decades have seen more oil spill incidences than ever before, except in war (Gulf War, 1991) situations.¹ Increasing oil spill accidents pollute oceans on daily basis causing severe complications to ecosystem, in particular proving catastrophic to native marine wildlife. Constant dissipation or scattering of oil into the marine environment over time has been proven deadly to marine life such as fish, birds, invertebrates, mammals, reptiles, plants and algae. One accident could leave a huge quantity of oil being split into one place inducing long-lasting impact on the environment.²⁻⁴

On the other hand, numerous terrestrial activities including industrial oily wastewater discharge, oil refineries, automotive industrial release, shipping travel, domestic drains and dumping cause lasting impact on day-to-day life of sweet water reservoir.⁵⁻⁷ Continuing deep water horizon oil spill accidents and their aftermath prompts robust and cleaner approaches.⁸ Also, there are issues surrounding stable emulsions, which pose serious challenges to meet desired specification for oil content in the product water or vice versa. Use of demulsifiers additives to attain high quality water increases operational cost in addition to demand for post recovery step.

On the other hand, researchers have been constantly looking for new materials and techniques to solve problems that are frightening our environment. In a unique attempt, nanoporous PTFE were used for the separation of two immiscible liquids based on the segmented flow microchemistry principle. Selective wettability resulted in successful separation of aqueous-organic/flourous liquid mixtures.⁹ Recently, detailed review has been reported highlighting advanced membranes used for separation of complex emulsified oil/water mixtures and effluents.¹⁰ Ceramic membrane in the ultrafiltration (UF) and microfiltration (MF) range have been developed to successful separation of both immiscible effluents and complex emulsions. Among all, $\text{Cu}(\text{OH})_2$ nanowire-haired membranes yielded as high as $\sim 100000 \text{ L.m}^{-2}.\text{h}^{-1}$.¹¹ On the other hand, ultrafast

^aScale-Up & Process Engineering Unit Discipline, CSIR-Central Salt & Marine Chemicals Research Institute, G. B Marg, Bhavnagar-364002 (Gujarat), India, Phone No :+91-278-2567760. Fax No: +91-278-2567562. Email:rmeena@csmcri.org

^bRO-Division, CSIR-Central Salt & Marine Chemicals Research Institute, G. B Marg, Bhavnagar-364002 (Gujarat), India. Email:sknata@gmail.com; sknataraj@csmcri.org

Electronic Supplementary Information (ESI) available: [supplementary information contains membrane swelling study results, long term performance in crossflow module and membrane surface generated images].

See DOI: 10.1039/b000000x/

separation of stable emulsions were achieved using carbon nanotube (CNT)-based membranes. With different set of membranes >96% purity to oil was achieved.¹² Hydro-responsive membrane prepared with simple dip-coating technique. Polyester fabric dip-coated using an organosilicon (f-POSS) in combination with cross-linked poly(ethylene glycol) diacrylate (x-PEGDA) resulting variable surface characteristics. As prepared flexible fabrics were successfully tested for both oil-in-water and water-in-oil emulsion separation applications.¹³

In addition to this, conventional electrospun polyacrylonitrile (PAN)-based nanofibrous membranes¹⁴ and solution cast polyvinylidene fluoride (PVDF) membrane having pore structures in the range of UF regime have been reported with reasonable product flux.¹⁵ General shortcoming with above mentioned membranes is that they suffer from poor mechanical properties and material integrity under applied pressure and continuous flow test conditions. In recent report, the development of ceramic coated mesh membranes has been successfully tested for oil-water separation. Composite ceramic membranes have shown exceptional ability to concentrate oily wastewater. High mechanical stability makes them a valuable, cost-effective alternative compare to traditional treatment methods.¹⁶

Here, we demonstrate a novel bio-based polycocolloid foam membrane (FM) ($\theta_{\text{water}} \approx 0^\circ$) prepared by blending agarose (Agr), gelatin (Gel) and genipin (G). All the constituents are bio-origin, easy to prepare and economical to extract. In addition, the main characteristic constituent crosslinker genipin is a non-toxic fruit extract. FMs have been tested both under gravity as well as accelerated crossflow membrane modules. Oily phase was retained in feed stream as superhydrophilic microporous membrane allowed selective separation of water to permeate side. With this, high degree of oil removal achieved through environmentally benign materials and cost effective process.

2. Experimental Section

2.1 Materials

Agarose, a hydrophilic phycolloid was extracted from red seaweed *Gracilaria dura* following the method reported and the gel strength, sulphate and ash contents of the agarose were >1900 g cm⁻² (1.0 % gel), ≤0.25% and 0.9%.¹⁷ Gelatin was purchased from NICE Chemicals Pvt. Ltd. COCHIN, and Genipin was purchased from Challenge Bioproducts Co. Ltd., Taiwan. All other chemicals were used as received without further purification.

2.2 Preparation of Membrane

In a beaker having 75 ml distilled water, agarose (1800 mg) was added under stirring condition and autoclave it at 120 °C for 15 min for complete solubilisation. In another beaker 200 mg gelatin in 25 ml distilled water was stirred to form homogenous solution (Figure 1). Then gelatin solution was added to the viscous agarose solution under vigorous stirring condition for 10 min at 70 °C to make complete blending. Then

genipin (10-40 mg dissolved in minimum amount of methanol) was added with continuous stirring at 50 °C and gradually cooled to room temperature to form hydrogel. After 10 min, the colour of whole solution starts changing from transparent to light blue colour due to the cross linking and resulting hydrogel was left for 7-10 days at room temperature for complete gel formation. After that each gel was cut to 0.4 mm thick slices and lyophilized at a freeze-drying temperature of -85 °C under vacuum to obtain porous foam membrane. The lyophilisation is one of the most common methods to induce porosity in the scaffolds leaving behind the porous structures.¹⁸ Different compositions of membranes were also prepared by changing the concentration agarose and gelatin ratios in the similar manner and tested for their oil/water separation performances.

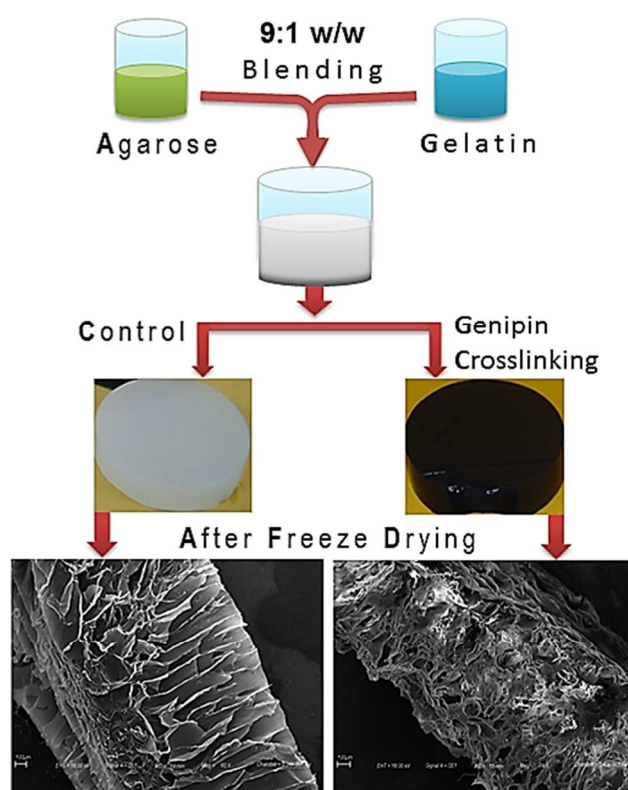


Figure 1. Schematic representation of FM preparation steps. Agarose and gelatin were blended in 9:1 w/w ratio and then genipin was added to crosslink the sample at 50°C. Solution turns to gel at room temperature; here figure shows gels with and without crosslinking agent (genipin) to elaborate the difference. Upon slicing, gels were subjected to freeze drying to yield porous bio-based foam membranes.

2.3 Membrane Testing

Foam membranes have been tested in two different configurations. Initial lab-scale tests were conducted under driving force of gravity. Gravity separation process is a simple and conventional separation process which makes use of density difference between two immiscible oil-water feed mixtures. For this, we used glass apparatus to monitor the separation process. One typical arrangement contains funnel

packed with FM to separate two chambers. Samples were poured in to funnel fitted with membrane and filtrate was collected at the bottom. Number of oil/water mixtures namely crude oil/water, hexane/water, toluene/water mixtures and real oil spill samples were tested in a similar procedure. Separation process was monitored for its permeation rate and purity. Permeate was analysed for its purity as mentioned in method section.

To check the emulsion break point, foam membranes were tested using crossflow membrane. Crossflow testing unit comprises of hollow chamber with inlet and outlet connected to a sustained crossflow velocity of the feed mixture. Booster pump was used to circulate oil/water mixture in to feed chamber. Each permeate sample was analyzed for its flux and rejection.

2.4 Methods

Autoclaving of samples was carried out by using Autoclave ES-315, (TOMY SEIKO CO., LTD, JAPAN). FTIR spectra were recorded on a Perkin-Elmer FTIR machine (Spectrum GX, USA). The surface morphology of the control and crosslinked agarose products was analyzed by scanning electron microscopy (SEM) on a Carl-Zeiss Leo VP 1430 instrument (Oxford INCA). Lyophilisation of gel samples was carried out using VirTis Benchtop, Freeze dryer, United States. Thermogravimetric analysis (TGA) was carried out using Mettler Toledo Thermal Analyzer, (TGA/SDTA 851e, Switzerland). The Solid state UV-vis spectra were measured using Shimadzu UV-3101PC spectrophotometer (JAPAN). ¹H-nuclear magnetic resonance (NMR) spectra were recorded on a Bruker Avance-II 500 (Ultra Shield, Switzerland) Spectrometer with DMSO as solvent and internal standard as well and Spectra were recorded at 70°C.

2.5. Permeate Flux and Rejection

The water flux (J) was calculated measuring quantity of water permeated across the FM every one hour interval and membrane area following equation:

$$J = \frac{V}{A \times t} \quad \dots\dots\dots (1)$$

Where, J is flux in ($L.m^{-2}.h^{-1}$), V volume of permeate collected at time t and A is area of the membrane.

The % rejected oil in permeate was calculated using equation:

$$\% R = \left(\frac{C_f - C_p}{C_p} \right) \times 100 \quad \dots\dots\dots (2)$$

Where, C_f and C_p are the concentration of feed and permeate solutions, respectively.

3. Results and Discussion

Agarose, a phycocolloid extracted from red seaweed with basic disaccharide repeating units consists of (1,3) linked α -D-galactose (G) and (1,4) linked β -L-3,6-anhydrogalactose (A). Agarose is well known for its hydrophilic nature and gelling behaviour. On the other hand, gelatin is full of amino-functional groups that are available for functionalization via crosslinking. So, blends of gelatin and agarose have attractive prospectus from scaffolds to films. From different approaches, gel can be converted to different morphological end product. In one such effort, we transformed agarose-gelatin gel to FM using genipin as crosslinking agent.

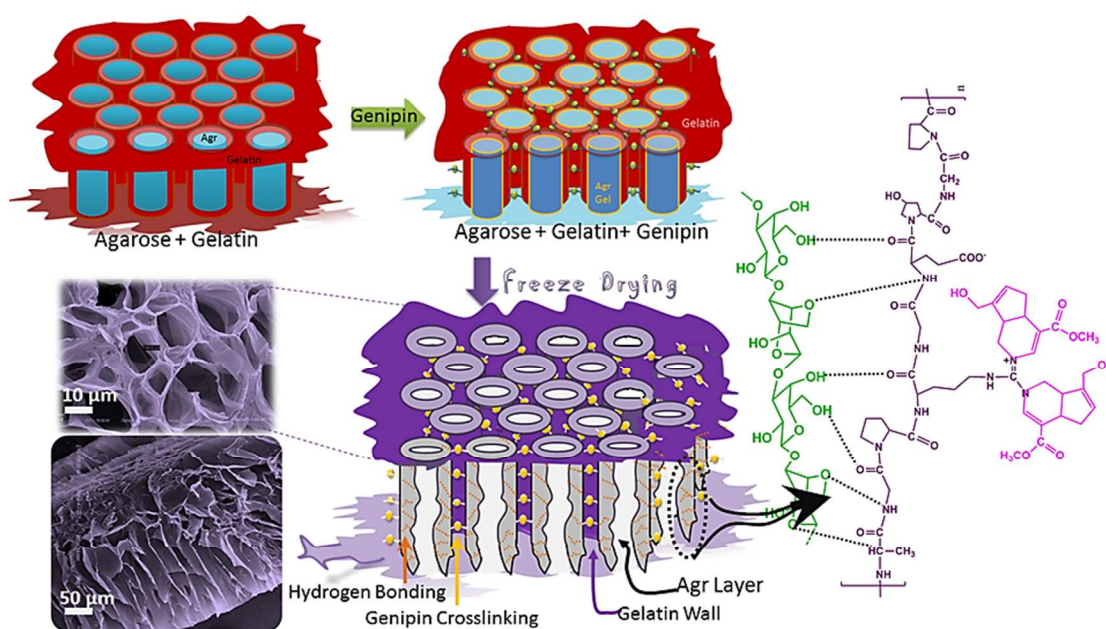


Figure 2. Scheme representing FM formation mechanism under the influence of genipin crosslinking and the hydrogen bonding interaction between agarose-gelatin co-gels. Crosslinking agent, time and freeze drying process drive the pore formation and their morphology in foam membranes.

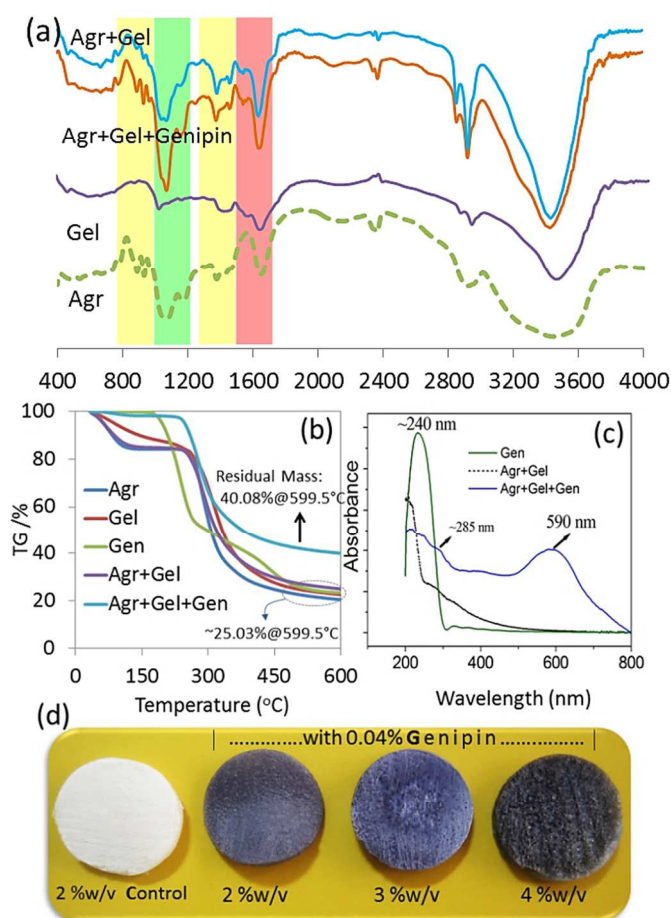


Figure 3. FTIR analysis of bio-based FM from pristine to final composition (a) Agr, Gel, Agr+Gel blend and genipin crosslinked Agr+Gel, (b) thermogravimetric analysis of pristine, blend and crosslinked FMs, (c) solid UV-spectroscopic measurement recorded on genipin powder, blend and crosslinked FM, and (d) actual photographic images of foam membrane, from control to crosslinked Agr+Gel with different blend concentration.

Figure 2 gives the detailed description of gelatin-agarose-based FM micropore formation mechanism and its morphology. When gelatin solution was added to the autoclaved agarose solution followed by stirring, stable blend was formed. Upon mixing followed by gradual cooling at room temperature, cylindrical aggregates of agarose soft chains phase separate in a non-crosslinked gelatin co-gel. With the addition of genipin, simultaneous conjugated interactions of crosslinkable amino groups within gelatin, hydrogen bonding between gelatin and agarose are initiated. As result, co-gel colour transforms in to blue soft matter.¹⁹ Once the genipin crosslinking completed gel was lyophilized. Under lyophilization ice crystals readily formed in agarose column assembly which then subjected to

sublimation process leaving behind porous voids and agarose layers on gelatin wall, which is regulated from hydrogen bonding.²⁰

To prove the proposed mechanism, membranes were extensively characterised for their characteristic changes using FTIR, TGA, solid UV analysis as well as NMR analysis. FTIR analysis in Figure 3(a), agarose exhibited characteristics peaks at 932 cm^{-1} (due to 3, 6-anhydrogalactose linkage), 1162 , 1076 cm^{-1} .¹⁷ Gelatin spectrum showed characteristic absorption bands at 3436 , 2925 , 1640 and 1530 cm^{-1} which corresponds to -OH, amine (N-H), amide I (C=O) and amide II (NH_2), respectively. Appearance of characteristics peaks in the FTIR spectrum of Ag+Gel+Gen confirms that the main characteristic absorption bands of agarose (1162 , 1076 and 932 cm^{-1}) remained intact during modification. However, characteristics bands of gelatin at 1640 , 1530 , 1240 cm^{-1} (due to amide linkage) also appear in final products. The main noticeable change appeared in the shift of broader Agr stretching peak (OH) at $\sim 3438\text{ cm}^{-1}$ upon blending with Gel ($\sim 3435\text{ cm}^{-1}$) to 3398 cm^{-1} . This remained unchanged upon genipin crosslinking. Therefore, hydroxyl (OH) groups present in agarose make hydrogen bonding interaction with N lone pair of the amide group of gelatin resulting in lamellar structure in which gelatin holding agarose either side. So, it leads to confirm that superhydrophilic agarose micro-pore is surrounded by gelatin walls used for selective separation from oil-water mixtures.

Further, thermogravimetric (TGA) and UV-visible spectroscopic tools were used to determine nature of membrane transformation and their stability. TGA results (see, **Figure 3(b)**) of the blend prepared in the presence of crosslinking agent showed the high thermal stability in comparison to pristine constituents. The minimum residual mass of 20.53% and $\sim 25\%$ was obtained for Agr and Agr+Gel blends, respectively. However, genipin crosslinked blend (Agr+Gel+Gen) retained as high as 40.08% residual mass at 599.5°C . Therefore, it directly implies the rigid network as a result of genipin crosslinking in FM.²¹ Control and crosslinked blend FM samples were analysed using solid UV spectroscopy. In Figure 3(c), the pristine genipin in water exhibited characteristic peak at 240 nm , whereas, control Agr+Gel blend had none. However, genipin crosslinked blend (Agr-Gel+Gen) exhibited shift in the characteristic genipin peak to 280 nm with the appearance of additional peak at 590 nm . This confirms extended conjugation of genipin crosslinking which induces dark blue color to FMs seen at 590 nm .²² In addition to this, crosslinking of amino group was further confirmed by the

disappearance of amine proton in the ^1H NMR of crosslinked FMs which occurs in the range of 7-8 ppm (See ESI† Figure S1).

Further, membrane swelling ought to be stabilized before fixing them to the separation cell or crossflow set-up. We performed swelling study of FM with different crosslinking ratio of genipin added. As the adequate crosslinking strongly adds stability to microstructures, subsequently 0.01 %, 0.02 %, 0.03 %, 0.04 % and 0.05 % (*w/v*, with respect to total solution) genipin crosslinked blend membranes (2% *w/v*) were measured for their swelling properties in pure water and water-oil (80:20) mixtures. ESI† Figure S2 gives swelling behaviour of control, 0.01 %, 0.02 %, 0.03 %, 0.04 % and 0.05 % (*w/v*) genipin in constant 2 % *w/v* gelatin-agarose blend mixtures. Results showed that stable microstructure were yielded with 0.04 % (*w/v*) genipin crosslinked membrane with ~ 70 % swelling in both pure water and 20:80 oil-water mixtures in comparison 0.01 % , 0.02 % (>80 %) and 0.03 % (<60 %) added genipin resulting in a soft unstable membrane. Subsequently 0.05 % genipin crosslinked FM exhibited similar swelling as observed for 0.04 % genipin crosslinked FM.

Figure 3(d) gives the appearance and texture of crosslinked FMs with different blend concentration in comparison with pristine blend foam. It is also evident from the images that the microstructure in 2 % *w/v* blend membrane is more uniform and compact. With this, further experiments were designed to evaluate for their water selectivity and separation efficiency using optimized 0.04 % (*w/v*) genipin (2 % *w/v* blend) crosslinked membrane.

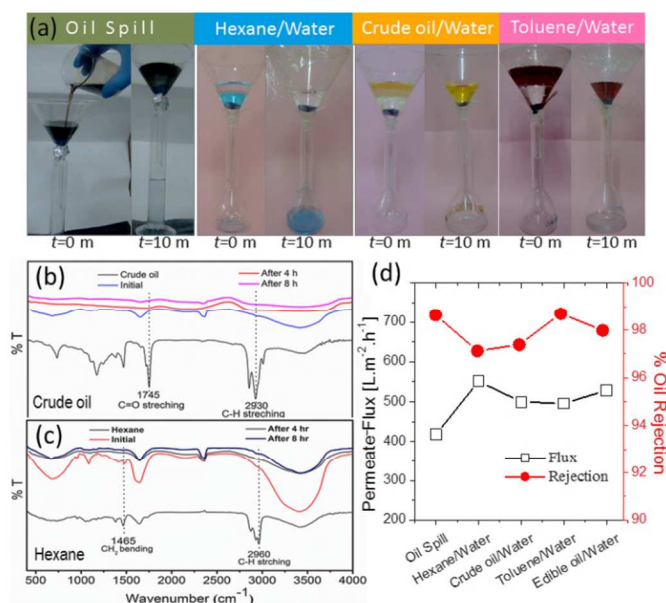


Figure 4. A gravity-driven oil-water separation apparatus with a 50:50 (*v/v*) oil-water mixtures. (a) Shows separation of oil spill and various oil-water mixture at lab scale, (b) Shows selective characterization of crude oil in permeate, disappearance of the characteristics peaks for C=O of esters and C-H stretching of oils respectively, (c) shows the characterization of hexane in permeate. (d) Displays the permeate flux ($\text{L}\cdot\text{m}^{-2}\cdot\text{h}^{-1}$) and % rejection of various oil/water mixtures.

Figure 4(a) gives characteristic photographic images of lab-scale experiments for oil-water separation conducted under gravity. Several oil-water mixtures were subjected to selective separation process under gravity as described in experimental section. Considering water as rich phase in permeate, infrared (IR) spectroscopy has been used as a tool to quantify the amount of oil diffused to permeate water. Prior to permeate sample analysis, we calibrated standard curve for different concentrations of oil-in-water. Six standard solutions over the range of 1 to 100 mg/L oil-in-water were prepared for stable emulsion using sonication bath. Further, these samples were subjected to FTIR analysis. Established calibration range fitted well with linearity and accuracy were observed with a correlation coefficient ($R^2=0.99957$) and a standard error of prediction of 0.247 mg/mL (please check) was obtained. Figure 4(b) Shows characterization of crude oil in permeate, disappearance of the characteristics peaks at 1745 and 2930 cm^{-1} (for C=O of esters and C-H stretching of oils respectively) indicates oil content in permeate is negligible. Figure 4(c) shows the characterizations of hexane in permeate disappearance of characteristic peaks at 1465, 2960 cm^{-1} for CH_2 bending and C-H stretching of hexane indicates that insignificant hexane diffused in to permeate. Similar results were also observed for oil spill, edible oil-water and toluene-water mixtures. Figure 4(d) Displays the permeate flux and % rejection of various mixtures namely, oil spill, hexane-water, crude oil-water, toluene-water and edible oil-water mixtures.

Concentration of oil-in-water calculated from Figure 4(b & c) were then plotted against permeate flux to correlate the membrane performance. It is evident that over 500 $\text{L}\cdot\text{m}^{-2}\cdot\text{h}^{-1}$ fluxes yielded with added >97 % purity to water. It is also important that the flux and rejections were identical and independent of feed nature.

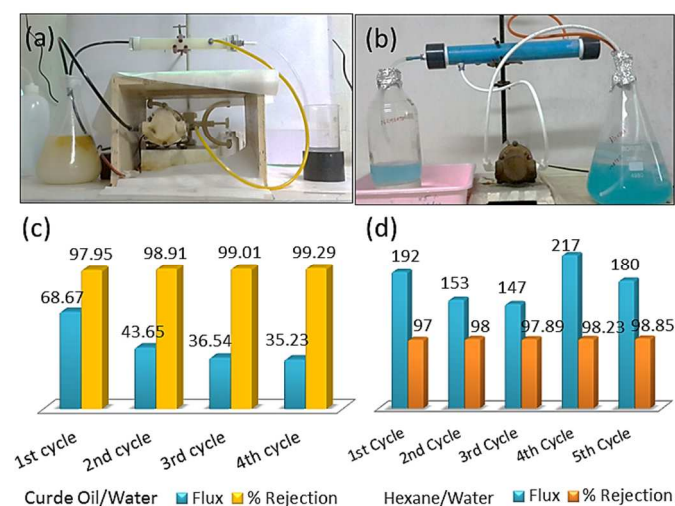


Figure 5. Photographs of actual crossflow experimental set-ups used for the separation of different oil-water emulsions in this study (a) gives snap shot of crude oil-water separation process, (b) hexane-water separation intermediate picture, (c) results of permeate flux and % rejection profiles from crude oil-water emulsions and (d) permeate flux and % rejection results from hexane-water emulsions tested at different cycle.

Separation of oil-water phases under gravity is a simple process and follows the principle of dead end filtration. In long terms it is expected that membrane not only passage water but also absorbs oil which reduces the separation selectivity and efficiency. In such situations, membrane performance can be accelerated by the assistance of cross flow pressure. Moreover in oil-in-water type emulsions, oil is the internal dispersed or discontinuous phase, while water is the external or continuous phase. Crossflow velocity and the continuous flow help membrane to enhance separation process. To test the efficiency membrane for their long term performance and stability, stable emulsion was pumped to feed chamber which lead continuous contact with feed and the membrane. Figure 5 (a) and (b) gives typical images of experimental set-ups used for several oil-water separation experiments (see Video File 1). In an oil-water emulsion, water molecules adsorb on the oil droplet forming in a stable suspension. When the emulsions were exposed to superhydrophilic FM water molecular film breaks resulting in a water droplets aggregate. Meanwhile, crossflow velocity of feed assist to drive the larger aggregated water droplets to pass through the bio-based FM pores leaving behind oil. Figure 5(c) and (d) gives complete assessment of foam membranes for their flux and rejection of crude oil and hexane from water rich streams.

As mentioned earlier membranes were tested under crossflow pressure (~ 0.2 bar) using crossflow velocity of feed. There has been substantial increase in rejection observed for both the mixtures. Even though initial cycles have shown similar results that of gravity separation but recorded substantial decline in flux. On the other hand, crude oil was rejected $>99\%$ later cycles (3rd and 4th cycle) for crude oil which remained constant for several repetitions. Interestingly, for hexane-water feed, rejection was stable to the point $\sim 98\%$ retaining substantial amount of permeate flux. It is also evident that the 4th and 5th cycles recovered initial flux over $200 \text{ L.m}^{-2}.\text{h}^{-1}$. Unlike dead end module, crossflow testing has revealed self-cleaning ability of foam membranes. It is significant phenomenon to note when transmembrane pressure is minimal, the capillary pressure prevents the oil from defusing into pore and the crossflow velocity clears the surface, preventing scale formation (Figure 6a). This significant phenomenon adds to more value to membrane life and the long term stability maintaining high rejection which satisfies the product water reuse and discharge norms.

Unlike traditional membrane processes which make use of dense or asymmetric micron-scale separating barrier, present study make use of foam membranes. It is likely that separated oil aggregates may accumulate on membrane developing a blocking layer for large extent. Also, in stable emulsified wastewater streams like oil spill samples suspended contaminants readily forms cake. With the self-cleaning nature of the foam membrane, with optimized crossflow run, fouling layer formation can be minimized. But, the same time columnar microstructures in membranes could collapse under crossflow pressure generated by the feed pump crossflow velocity. One

such experiment was conducted to check the surface morphology of the membrane which repeatedly exposed to oil/water mixture under pressure. Figure 6(b) gives SEM image of fouled membrane. After several runs, contaminated oil aggregates accumulate on the membrane surface. In such case, flux decline is inevitable (ESI† Figure S3) but can be minimized with suitable engineering adopted to protect membrane from direct flow impact.

Biodegradability factor

Preparing a biodegradable membrane was not only the desired target knowing nature of application, expected long term performance and economics involved. But, renewable resources which undergo biodegradability is an important aspect of sustainability. In such situation, intrinsic biodegradability factor of a new engineering material helps in balancing environmental issue associated with disposal after use. In our case, we tested membrane for its recyclability (ESI† Figure S2) and reuse after washing in simple soap water to remove adhered oil contaminants on membrane surface. By this way, foam membranes were repeatedly tested for their recyclability. In case of fouled membrane, material disposal also happened to be environmental friendly aspect as FM readily undergoes biodegradation process. Figure 6(c) illustrates a photograph where the FM is seen gradually undergoing degradation process. Oil-fouled FM was concealed in soil and biodegradation process was monitored constantly. After 5 and 10 days membrane status clearly shows the physical deformation induced by biodegradation process. More than 50% (w/w) weight loss has been recorded after 10 days. From the observations it is evident that in given favourable conditions, FM would readily undergo complete biodegradation process in 25-30 days' time, without hurting mother-nature.

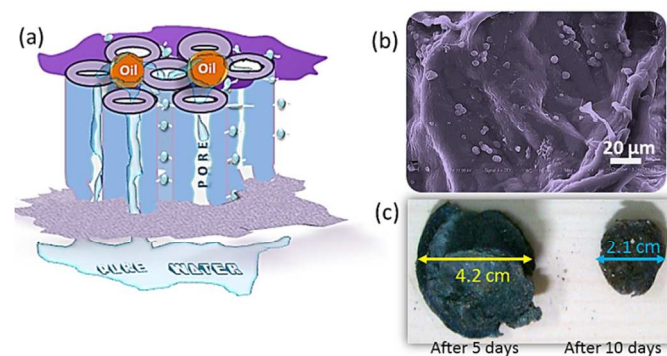


Figure 6. Performance of bio-based foam membrane (a) pure water transport through superhydrophilic ($\theta_{\text{water}} \approx 0$) channels leaving behind rejected oil (b) SEM with retained oil deposits on the oleophobic surface ($\theta_{\text{water}} > 150$), (c) Biodegraded foam membranes in soil examined after 5 days and after 10 days (about 50 weight loss was obtained).

4. Conclusions

In summary, present study demonstrates that microporous foam membranes have several advantageous properties with respect to their use in oil-water separation. The attractive properties of

foam membranes include natural abundance, less-to-no toxicity, stable under different testing conditions, easy to process and dispose. Biodegradability factor is a significant characteristic of the foam membrane which makes it eco-friendly separation medium in comparison to conventional materials and methods. Over 500 L.m⁻².h⁻¹ with ~98 % pure water is a promising feature of our microporous membrane. FM also works in an advanced crossflow configuration which opens new avenue to faster water reclamation process from large industrial streams. One of the prospectives focus using FM is to reclaim water from oil or gas exploration operations. On the other hand, oil-water emulsion wastes and oil sludge are easy to process through with improved rate of dewatering process. Therefore, water recovery using continuous filtration process using bio-based membranes is an economical and sustainable solution.

Acknowledgements

CSIR-CSMCRI communication number 056/2014. RM and JPC gratefully acknowledge DST, New Delhi, Government of India for financial support (SB/EMEQ-052/2013). SKN gratefully acknowledges the DST, Government of India for the DST-INSPIRE Fellowship and Research Grant (IFA12-CH-84).

Notes and references

1. S. E. Allan, B. W. Smith and K. A. Anderson, *Environ. Sci. Technol.*, 2012, **46**, 2033-2039.
2. C. Pérez, A. Velando, I. Munilla, M. López-Alonso and D. Oro, *I.S. E. Allan, B. W. Smith and K. A. Anderson, Environ. Sci. Technol.*, 2008, **42**, 707-713.
3. A. M. Bernabeu, D. Rey, B. Rubio, F. Vilas, C. Domínguez, J. M. Bayona and J. Albaigés, I. S. E. Allan, B. W. Smith and K. A. Anderson, *Environ. Sci. Technol.*, 2009, **43**, 2470-2475.
4. R. H. Carmichael, A. L. Jones, H. K. Patterson, W. C. Walton, A. Pérez-Huerta, E. B. Overton, M. Dailey and K. L. Willett, *I.S. E. Allan, B. W. Smith and K. A. Anderson, Environ. Sci. Technol.*, 2012, **46**, 12787-12795.
5. J. Rivas, A. R. Prazeres and F. Carvalho, *J. Agric. Food Chem.*, 2011, **59**, 2511-2517.
6. F. J. Rivas, O. Gimeno, J. R. Portela, E. M. de la Ossa and F. J. Beltrán, *Ind. Eng. Chem. Res.*, 2001, **40**, 3670-3674.
7. A. Asatekin and A. M. Mayes, *Environ. Sci. Technol.*, 2009, **43**, 4487-4492.
8. T. J. Crone and M. Tolstoy, *Science*, 2010, 330, 634.
9. J. H. Bannock, T. W. Phillips, A. M. Nightingale and J. C. deMello, *Anal. Methods.*, 2013, **5**, 4991-4998.
10. Y. Zhu, D. Wang, L. Jiang and J. Jin, *NPG Asia Mater.*, 2014, **6**, e101.
11. F. Zhang, W. B. Zhang, Z. Shi, D. Wang, J. Jin and L. Jiang, *Adv. Mater.*, 2013, **25**, 4192-4198.
12. Z. Shi, W. Zhang, F. Zhang, X. Liu, D. Wang, J. Jin and L. Jiang, *Adv. Mater.*, 2013, **25**, 2422-2427.
13. A. K. Kota, G. Kwon, W. Choi, J. M. Mabry and A. Tuteja, *Nat Commun.*, 2012, **3**, 1025.
14. K. Yoon, K. Kim, X. Wang, D. Fang, B. S. Hsiao and B. Chu, *Polymer*, 2006, **47**, 2434-2441.
15. W. Zhang, Z. Shi, F. Zhang, X. Liu, J. Jin and L. Jiang, *Adv. Mater.*, 2013, **25**, 2071-2076.
16. Q. Wen, J. Di, L. Jiang, J. Yu and R. Xu, *Chemical Science*, 2013, **4**, 591-595.
17. R. Meena, A. K. Siddhanta, K. Prasad, B. K. Ramavat, K. Eswaran, S. Thirupathi, M. Ganesan, V. A. Mantri and P. V. S. Rao, *Carbohydr. Polym.*, 2007, **69**, 179-188.
18. Q. L. Q. Feng, *J. Mater Sci: Mater Med.*, 2006, **17**, 1349-1356.
19. I. K. Touyama R., Takeda Y., Yatsuzuka M., Ikumoto T., Moritome N., Shingu T., Yokoi T., Intuye H, *Chem. Pharm. Bull.*, 1994, **42**, 1571-1578.
20. L.-W. Xia, R. Xie, X.-J. Ju, W. Wang, Q. Chen and L.-Y. Chu, *Nat Commun*, 2013, **4**. DOI: 10.1038/ncomms3226
21. D. Saravanan, T. Gomathi, P. N. Sudha, *Archives of Applied Science Research*, 2011, **3**, 342-350.
22. M. U. Chhatbar, R. Meena, K. Prasad, D. R. Chejara and A. K. Siddhanta, *Carbohydr. Res.*, 2011, **346**, 527-533.